Geoscience Frontiers 12 (2021) 81–92

HOSTED BY

Contents lists available at ScienceDirect

Geoscience Frontiers

journal homepage: www.elsevier.com/locate/gsf

Research Paper

PetroGram: An excel-based petrology program for modeling of magmatic processes

Mesut Gündüz [a,*], Kürşad Asan [b]

[a] Graduate School of Natural Sciences, Muğla Sıtkı Koçman University, TR-48000, Muğla, Turkey
[b] Geological Engineering Department, Konya Technical University, TR-42250, Konya, Turkey

ARTICLE INFO

Handling Editor: Stijn Glorie

Keywords:
PetroGram
Magmatic petrology
Geochemical modeling
Partial melting
Crystallization
Assimilation
Magma mixing

ABSTRACT

PetroGram is an Excel© based magmatic petrology program that generates numerical and graphical models. PetroGram can model the magmatic processes such as melting, crystallization, assimilation and magma mixing based on the trace element and isotopic data. The program can produce both inverse and forward geochemical models for melting processes (e.g. forward model for batch, fractional and dynamic melting, and inverse model for batch and dynamic melting). However, the program uses a forward modeling approach for magma differentiation processes such as crystallization (EC: Equilibruim Crystallization, FC: Fractional Crystallization, IFC: Imperfect Fractional Crystallization and In-situ Crystallization), assimilation (AFC: Assimilation Fractional Crystallization, Decoupled FC-A: Decoupled Fractional Crystallization and Assimillation, A-IFC: Assimilation and Imperfect Fractional Crystallization) and magma mixing. One of the most important advantages of the program is that the melt composition obtained from any partial melting model can be used as a starting composition of the crystallization, assimilation and magma mixing. In addition, PetroGram is able to carry out the classification, tectonic setting, multi-element (spider) and isotope correlation diagrams, and basic calculations including Mg#, Eu/Eu*, ε_{Sr} and ε_{Nd} widely used in magmatic petrology.

1. Introduction

The chemical composition of magmatic rocks is controlled by a number of petrological processes such as melting, crystallization, assimilation, magma mixing. Although technical advances have dramatically increased our ability to analyze the chemical composition of magmatic rocks and to identify the role of these processes in their genesis and evolution, the need for computer programs producing quantitative models has become increasingly important. There are several complimentary or commercial computer programs such as FC-Modeler (Keskin, 2002), PetroPlot (Su et al., 2003), GCDkit (Janoušek et al., 2003, 2006), GeoKit (Lu, 2004), PetroGraph (Petrelli et al., 2005), GeoPlot (Zhou and Li, 2006), GCDPlot (Wang et al., 2008), FC-AFC-FCA and mixing modeler (Ersoy and Helvacı, 2010), PETROMODELER (Ersoy, 2013), AFC-Modeler (Keskin, 2013), GeoPyTool (Yu et al., 2019) and IgPet (RockWare®) to produce petrological models and geochemical plots. MELTS (Ghiorso and Sack, 1995; Asimow and Ghiorso, 1998) and Petrolog (Danyushevsky and Plechov, 2011) represent another class of computer programs designed to facilitate thermodynamic modeling of phase equilibria in magmatic systems. For the petrological processes mentioned above, except IgPet, these computer programs do not either include any petrological modeling option or only use a forward modeling approach. Forward models are thought to be complex requiring more parameters which govern the petrological process such as melting degree, initial source concentrations and partition coefficients. However, inverse geochemical models are simple models reducing the number of parameters, and have attracted more attention in igneous petrology during last years because of involving deciphering information from the measured elemental abundances and isotope compositions (Zou, 2007).

Here we have developed an Excel-based magmatic petrology program called PetroGram which can produce petrological models based on both forward and inverse geochemical modeling that is not included in the existing programs mentioned above by using whole-rock major oxides, trace elements and isotopes. The program is also able to carry out the classical diagrams for magmatic rock classification, tectonic setting, multi-element (spider), isotope correlations (e.g. epsilon values (ε) and initial ratios (i) for Nd, Hf, Sr isotopes and depleted mantle model ages for Nd and Hf isotopes) and basic geochemical calculations widely used

* Corresponding author.
E-mail address: mesutgunduz24@hotmail.com (M. Gündüz).
Peer-review under responsibility of China University of Geosciences (Beijing).

https://doi.org/10.1016/j.gsf.2020.06.010
Received 23 September 2019; Received in revised form 16 April 2020; Accepted 10 June 2020
Available online 7 August 2020

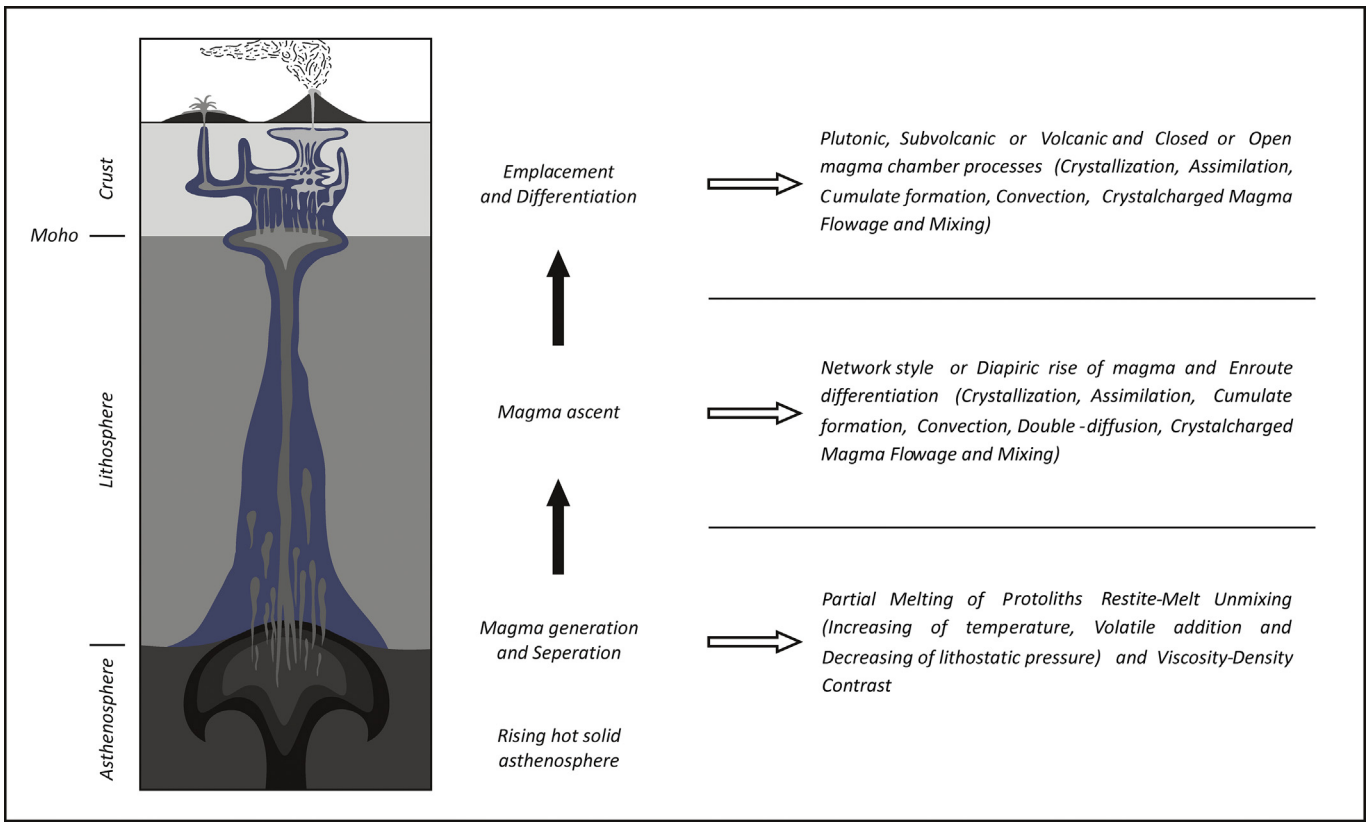

Fig. 1. Schematic diagram summarizing the generation, migration, emplacement and differentiation of magma (after Marshak, 2008; Kumar, 2014).

in magmatic petrology. Therefore, we think that PetroGram is very useful for teaching conceptual problems in igneous petrology to graduate students. The more advanced researchers can also benefit from the program to some extent. This paper is organised as two main sections: the first section focuses on "Magmatic Processes" giving a theoretical perspective. The second section deals with "Program Structure" describing how to use the program with worked examples. PetroGram runs on all Excel versions running under any Windows configuration, and occupies around 21 MB disk space.

2. Magmatic processes

Magmas are commonly high-temperature silicate melts of wide compositional range from ultrabasic to acidic types, and generated by partial melting of upper mantle (e.g. McKenzie and Bickle, 1988) or crust (e.g. Annen et al., 2008). The composition of a melt is determined by the mineralogy and chemistry of the source rock, type of melting process and degree of partial melting. Possible ways in which partial melting may occur are lowering of pressure or decompression (e.g. mid-ocean ridge basalt-MORB from oceanic rift, ocean island basalt-OIB from mantle plume and continental flood basalt-CFB from continental rift), addition of fluid phases or flux melting (e.g. arc basalt from subduction zone) and increasing in temperature (e.g. granite from collision or subduction zone). Magmas generated in the Earth's mantle have lower density compared to surrounding rocks, and generally rise to the Moho discontinuity which represents the transition from mantle to crust, and also known as "magma underplating". The melt fraction must increase sufficiently to overcome the surface free energy in order to segregate from magma source, but for some basaltic magmas, very small melt fractions can be removed from their source region (McKenzie, 1985b). However, some magmas can directly inject into the crust without stalling at the Moho as in kimberlites due to their lower viscosities and higher buoyancies that enable exceptionally rapid transport from the source region (Kamenetsky et al., 2011). The density contrast is an important factor to rise magma, but this cannot be only factor and dynamic factors are likely to be involved as well for the rise of a magma. Other factors are exsolution and expansion of bubbles in volatile-saturated magmas, and magma overpressure (Marrett and Emerman, 1992). Magmas generally form reservoirs as trans-crustal magma chambers at the base of crust to the shallow level before reaching the Earth's surface. Changing the composition of the primitive parental magmas, differentiation takes place in these chambers. Fractional crystallization (FC) is one of the most powerful mechanism in magmatic differentiation where early-crystallized minerals are assumed to become isolated from the residual melt and accumulate on the floor or walls of the magma chamber as "cumulates" (e.g. the Kilaeua Iki lava lake; Helz, 1980). In fractional crystallization, the cumulate mineral assemblage comprises plutonic rocks, but volcanic rocks represent a minute fraction of residual melt that have escaped to the surface. Although cumulate-forming process may be inhibited due to high viscosity in SiO_2-rich-felsic magmas, crystallization on the side walls may result in the accumulation of crystalline materials at the margin of the felsic magma chamber and generates highly evolved melts as in in-situ crystallization. Mixing and assimilation of wall-rocks are the other processes significantly changing the composition of magmas. Assimilation coupled with fractional crystallization (AFC) can be an important process in the evolution of much continental magmas (e.g. the Pikes Peak batholith; Barker et al., 1975). On the other hand, mixing can be viewed as replenishment of magma chambers by new pulses of magma (e.g. Palisades sill; Shirley, 1987) or mixing between different batch of mafic-felsic magmas (e.g. the central Sierra Nevada batholith; Barbarin, 2005). Taken as a whole, crystallization, magma mixing and assimilation are important differentiation processes operating either separately or commonly in combination in magma chambers (Fig. 1). Here we briefly summarized the main magmatic processes from the solid source through ascent to emplacement in the crust or eruption onto the surface, all can be petrologically modelled by PetroGram using

Table 1
Definition of terms used in equations for models.

C_0	Concentration of a trace element in the original unmelted solid source rock in melting or initial trace element concentration of the parental magma in fractional crystallization
C_a	Concentration of an element in the assimilating wall-rock material in AFC and A-IFC
C_f	Result of the fractional crystallization in decoupled assimilation-fractional crystallization
$\boldsymbol{C_I}$	Concentration of a trace element in instantaneous melt
$\boldsymbol{C_L}$	Concentration of a trace element in accumulated melt
$\boldsymbol{C_l}$	Concentration of a trace element in the liquid produced in crystallization
C_A, C_B	Concentrations of element A and B of melt in inverse melting and magma mixing
$\boldsymbol{C_A^0}, \boldsymbol{C_B^0}$	Source rock element concentrations of inverse batch melting and inverse dynamic melting
$\boldsymbol{C_S}, \boldsymbol{C_R}$	Concentration of a trace element in the residual solid and total residual, respectively after melting
C_A, IC_A, C_B, IC_B	Elemental concentrations and isotope ratios of the end-member A and B, respectively in magma mixing
C_m^0, C_l^0, C_x^0	Original (initial) concentration of an element in the magma, liquid and suspended crystals, respectively in A-IFC
$\boldsymbol{C_m^{A\text{-}IFC}}, \boldsymbol{C_l^{A\text{-}IFC}}, \boldsymbol{C_x^{A\text{-}IFC}}$	Concentration of an element in the magma, liquid and suspended crystals, respectively in A-IFC
$\boldsymbol{C_\eta}, \boldsymbol{IC_q}$	Elemental concentration and isotope ratio in two-component mixture, respectively in magma mixing
D	Bulk partition coefficient of the fractionating assemblage during crystallization or bulk partition coefficient of the original solids in during melting
F	Weight fraction of liquid produced in melting or the fraction of melt remaining in fractional crystallization
f	Fraction of the melt that returns to the magma chamber out of the solidification zone in In-situ crystallization
IC_0, IC_a	Isotope ratios of the melt and assimilated material, respectively in AFC
$\delta C_0, \delta C_a$	Stable isotope concentrations of the melt and assimilated material, respectively in AFC
Kd	Partition coefficient of an element in a mineral phase
m_a, m_c	Mass of the assimilated and crystallized material, respectively in AFC
M_c	Mass of the solid removed in decoupled assimilation-fractional crystallization
P	Bulk partition coefficient of the minerals entering the melt in non-modal melting
$\boldsymbol{Q_A}, \boldsymbol{Q_B}$	Ratio of highly incompatible element (A) to less incompatible element (B) in inverse melting
r, r_a	Ratio of the assimilation rate to the crystal fractionation rate in AFC and A-IFC, respectively
X	Percentage of melt fraction in dynamic melting or mixing fraction in magma mixing
δ	Weight fraction of the suspended crystals in imperfect fractional crystallization and A-IFC
$\varepsilon_m^0, \varepsilon_l^0, \varepsilon_x^0$	Original (initial) isotopic ratio of the magma, liquid and suspended crystals, respectively in A-IFC
$\boldsymbol{\varepsilon_m}, \boldsymbol{\varepsilon_l}, \boldsymbol{\varepsilon_x}, \varepsilon_a$	Isotope ratios in the magma, liquid, suspended crystals and anatectic wall-rock melt, respectively in A-IFC
ρ_f, ρ_s	Density of melt and solid, respectively in dynamic melting
ϕ_m, ϕ_v	Mass and volume porosity, respectively in dynamic melting
Δ	Mineral-melt fractionation factor for stable isotope

Output parameters in equations are shown as bold, input parameters as normal.

geochemical data.

Partition coefficient (Kd) is one of the most important geochemical parameters to model magmatic processes. It is defined as the ratio of concentration of trace element in the solid phase (i.e. mineral) to that in the liquid phase (i.e. melt). Therefore, the partition coefficients are used in the description of many petrological phenomena from partial melting to crystallization and assimilation. Bulk partition coefficient is calculated by

$$D = x_a \times Kd_a + x_b \times Kd_b + \ldots + x_n \times Kd_n \quad (1)$$

where D is the bulk partition coefficient, x is the weight fraction of the mineral phase and Kd is the partition coefficient of any element in mineral phase (Table 1).

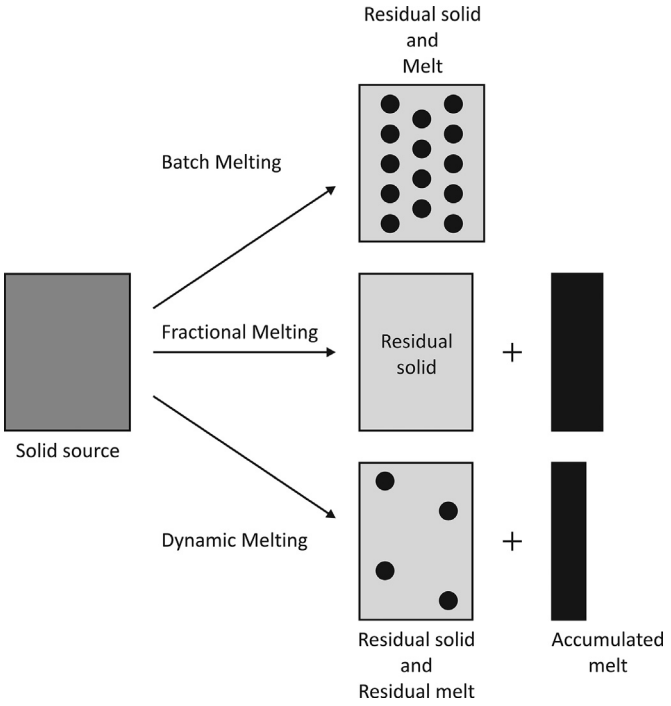

Fig. 2. Diagram showing batch, fractional and dynamic melting models (after Zou, 2007).

2.1. Partial melting

Partial melting can be modelled by both forward and inverse geochemical approach. There are three different forward (Fig. 2) and two different inverse partial melting models based on the geochemical equilibrium between the solid source and melt (Zou, 2007). Forward partial melting models can be classified as the forward batch melting model, forward fractional melting model (Schilling and Winchester, 1967; Gast, 1968; Shaw, 1970) and forward dynamic melting model (Langmuir et al., 1977; McKenzie, 1985a; Zou, 1998, 2000; Zou and Reid, 2001).

These forward partial melting models are divided into two sub-types: "modal" (non-common melting type) and "non-modal" (common type of fusion). In the case of modal melting, when any solid source rock undergoes partial melting, the minerals undergoing melting are proportional to the primary modal mineralogical composition. But, the mineral proportions in the melt are different from the source in non-modal (eutectic) melting models (Wilson, 1989; Rollinson, 1993). Bulk partition coefficient of the trace element of the minerals entering the melt is calculated by

$$P = y_a \times Kd_a + y_b \times Kd_b + \ldots + y_n \times Kd_n \quad (2)$$

where, P is the weight fraction of the mineral entering the melt phase, y is the weight fraction of the mineral phase and Kd is the partition coefficient of any element in mineral phase.

Two different types of inverse modeling are treated in PetroGram; inverse batch melting (IBM) and inverse dynamic melting (IDM). Inverse modeling is highly important and useful for gechemical investigations. The aim of inverse geochemical modeling is to approach the source rock geochemistry before partial melting by selecting suitable samples (Zou and Zindler, 1996; Zou, 2007). Inverse geochemical models are very useful to investigate of element abundance in source rocks because geochemical investigations generally are based on the element abudance

and isotope compositions (Zou, 2007). However, results of inverse geochemical models can not be used to create forward geochemical models (e.g. crystallization, assimilation and mixing) because they are higly complex models, and contain more parameters than inverse geochemical models.

2.1.1. Forward batch melting

Melt maintains chemical equilibrium with solid, and stays with solid until the final extraction during batch melting (Zou, 2007). It is more effective during partial melting of the crustal rocks, in which more viscous, felsic melts with higher permeability threshold are produced (Rollinson, 1993). Modal batch melting can be modelled as instantaneous C_I^{BM} or accumulated C_L^{BM} by using

$$C_I^{BM} = C_L^{BM} = \frac{C_0}{F + D(1-F)} = \frac{C_0}{D + F(1-D)} \tag{3}$$

Non-modal batch melting can be modelled as instantaneous C_I^{BM} or accumulated C_L^{BM} by using

$$C_I^{BM} = C_L^{BM} = \frac{C_0}{D + F(1-P)} \tag{4}$$

Modal batch melting residual solid C_S^{BM} and total residual C_R^{BM} can be modelled by using

$$C_S^{BM} = C_R^{BM} = \frac{DC_0}{D + F(1-D)} \tag{5}$$

Non-modal batch melting residual solid C_S^{BM} and total residual C_R^{BM} can be modelled by using

$$C_S^{BM} = C_R^{BM} = \frac{D - FP}{1-F}\frac{C_0}{D + F(1-P)} \tag{6}$$

C_0 is the concentration of the trace element in the source rock (starting composition), F is the fraction (%) of liquid produced during melting.

2.1.2. Forward fractional melting

Melt is extracted as soon as it is generated, and only the last drop of extracted melt is in equilibrium with the solid during fractional melting (Wilson, 1989; Zou, 2007). Modal fractional melting can be modelled as instantaneous C_I^{FM} or accumulated C_L^{FM} by using

$$C_I^{FM} = \frac{C_0}{D}(1-F)^{\frac{1}{D}-1} \tag{7}$$

$$C_L^{FM} = \frac{C_0}{F}\left(1-(1-F)^{\frac{1}{D}}\right) \tag{8}$$

Non-modal fractional melting can be modelled as instantaneous C_I^{FM} or accumulated C_L^{FM} by using

$$C_I^{FM} = \frac{C_0}{D}\left(1-\frac{FP}{D}\right)^{\frac{1}{P}-1} \tag{9}$$

$$C_L^{FM} = \frac{C_0}{F}\left(1-\left(1-\frac{FP}{D}\right)^{\frac{1}{P}}\right) \tag{10}$$

Modal fractional melting residual solid C_S^{FM} and total residual C_R^{FM} can be modelled by using

$$C_S^{FM} = C_R^{FM} = C_0(1-F)^{\frac{1}{D}-1} \tag{11}$$

Non-modal fractional melting residual solid C_S^{FM} and total residual C_R^{FM} can be modelled by using

$$C_S^{FM} = C_R^{FM} = \frac{C_0}{1-F}\left(1-\frac{FP}{D}\right)^{\frac{1}{P}} \tag{12}$$

2.1.3. Forward dynamic melting

In the dynamic melting model, the extracted melt is in equilibrium with the solid source until the critical value. When the degree of partial melting is greater than the critical value, any extra melt is extracted (Shaw, 2000; Zou, 2007). Modal dynamic melting can be modelled as instantaneous C_I^{DM} or accumulated C_L^{DM} by using formula following

$$C_I^{DM} = \frac{C_0}{\phi_m + (1-\phi_m)D}(1-X)^{\frac{1}{\phi_m+(1-\phi_m)D}-1} \tag{13}$$

$$C_L^{DM} = \frac{C_0}{X}\left(1-(1-X)^{\frac{1}{\phi_m+(1-\phi_m)D}}\right) \tag{14}$$

The mass porosity (ϕ_m) and percentage of melt fraction (X) to be left behind (i.e. trapped melt) in the residual rock are calculated in order to create dynamic melting model. Mantle melting frequently invokes porosity which controls the velocity of the melt relative to the solid, and the rate of melting and volume porosity are constant and finite in dynamic melting (McKenzie, 1984; Sims et al., 1999).

$$\phi_m = \frac{\rho_f\phi_v}{\rho_f\phi_v + \rho_s(1-\phi_v)} \tag{15}$$

$$X = \frac{F-\phi_m}{1-\phi_m} \tag{16}$$

where ϕ_v is the volume porosity, ρ_f is the density of melt, ρ_s is the density of solid.

Non-modal dynamic melting can be modelled as instantaneous C_I^{DM} or accumulated C_L^{DM} by using

$$C_I^{DM} = \frac{C_0}{D+\phi_m(1-P)}\left(1-\frac{X(P+\phi_m(1-P))}{D+\phi_m(1-P)}\right)^{\frac{1}{\phi_m+(1-\phi_m)P}-1} \tag{17}$$

$$C_L^{DM} = \frac{C_0}{X}\left(1-\left(1-\frac{X(P+\phi_m(1-P))}{D+\phi_m(1-P)}\right)^{\frac{1}{\phi_m+(1-\phi_m)P}}\right) \tag{18}$$

Modal dynamic melting residual solid C_S^{DM} and total residual C_R^{DM} can be modelled by using

$$C_S^{DM} = DC_I^{DM} \tag{19}$$

$$C_R^{DM} = \phi_m C_I^{DM} + (1-\phi_m)C_S^{DM} \tag{20}$$

Non-modal dynamic melting residual solid C_S^{DM} and total residual C_R^{DM} can be modelled by using

$$C_S^{DM} = \frac{D-P(X+\phi_m(1-X))}{(1-X)(1-\phi_m)}C_I^{DM} \tag{21}$$

$$C_R^{DM} = (1-\phi_m)C_S^{DM} + \phi_m C_I^{DM} \tag{22}$$

2.1.4. Inverse batch melting

In the batch melting, concentrations of elements in the melt (C_A and C_B) are calculated for highly incompatible element-A and less incompatible element-B by using

$$C_A = \frac{C_A^0}{D_A + F(1-P_A)} \tag{23}$$

$$C_B = \frac{C_B^0}{D_B + F(1 - P_B)} \tag{24}$$

F_1 and F_2 are melt fractions, and enrichment ratio of low-F/high-F for highly incompatible elements (Q_A) and less incompatible elements (Q_B) are calculated by using

$$Q_A = \frac{C_A^1}{C_A^2} = \frac{D_A + F_2(1 - P_A)}{D_A + F_1(1 - P_A)} \tag{25}$$

$$Q_B = \frac{C_B^1}{C_B^2} = \frac{D_B + F_2(1 - P_B)}{D_B + F_1(1 - P_B)} \tag{26}$$

F_1 and F_2 values can be solved from the system of the above equations based on the approximation of Maaløue (1994). But, Zou and Zindler (1996) argued that this approximation is specific, and they proposed other formulations: F_1 and F_2 are calculated for the batch melting as follow,

$$F_1 = \frac{D_A(1 - P_B)(1 - Q_A) - D_B(1 - P_A)(1 - Q_B)}{(Q_A - Q_B)(1 - P_A)(1 - P_B)} \tag{27}$$

$$F_2 = \frac{Q_B(D_B + F_1(1 - P_B)) - D_B}{1 - P_B} \tag{28}$$

2.1.5. Inverse dynamic melting

Enrichment ratio of low-F/high-F for highly incompatible elements (Q_A) and less incompatible elements (Q_B) are calculated by using following equations (Zou and Zindler, 1996; Zou, 2000),

$$Q_A = \frac{C_A^1}{C_A^2} = \frac{X_2}{X_1} \frac{1 - (1 - X_1)^{1/(\phi_m + (1 - \phi_m)D_A)}}{1 - (1 - X_2)^{1/(\phi_m + (1 - \phi_m)D_A)}} \tag{29}$$

$$Q_B = \frac{C_B^1}{C_B^2} = \frac{X_2}{X_1} \frac{1 - (1 - X_1)^{1/(\phi_m + (1 - \phi_m)D_B)}}{1 - (1 - X_2)^{1/(\phi_m + (1 - \phi_m)D_B)}} \tag{30}$$

For the equation, both highly incompatible and less incompatible elements have to be selected because these elements have different enrichment rates (Q) in magmas generated by different degrees of partial melting. The important feature of Q_A and Q_B is that they are independent of the source concentration (Q_0). The formulas form series of nonlinear equations with two unknowns as X_1 and X_2. These can be solved by Newton-Raphson's system of nonlinear equations (see "worked examples").

F_1 and F_2 calculated from the concentration method for inverse batch melting (IBM), can be used as a good initial estimate for the numerical solution of the equation system in the inverse dynamic melting model (IDM) (Zou, 2007). After obtaining X_1 and X_2, the partial melting degree (F) can be calculated by using

$$F = \phi_m + (1 - \phi_m)X \tag{31}$$

Inverse dynamic melting model, the source concentration can be calculated by using

$$C_A^0 = \frac{C_A X}{1 - (1 - X)^{1/(\phi_m + (1 - \phi_m)D_A)}} \tag{32}$$

$$C_B^0 = \frac{C_B X}{1 - (1 - X)^{1/(\phi_m + (1 - \phi_m)D_B)}} \tag{33}$$

2.2. Crystallization and assimilation

Crystallization takes place as temperature falls in magma, resulting in the formation of solid mineral phases and changing in the composition of melt. Crystallization models given here are treated as closed (i.e. no material exchange) and the proportions of mineral crystallizing and partition coefficients are constant (Shaw, 2006). Assimilation is an open-system differentiation in the magma chamber. While magma rises from deeper to shallow crustal levels, it can change the composition by dissolving the wall rocks.

C_0 is the initial trace element composition of the magma, D is the bulk partition coefficient in the all crystallization and assimilation processes. F is defined as the fraction (%) of the initial magma remaining after fractional crystallization (Zou, 2007).

2.2.1. Equilibrium crystallization

During equilibrium crystallization, crystals continuously react and re-equilibrate completely with melt as pressure, temperature and composition change. The physical process leading to equilibrium crystallization is the condition that solid-state diffusion in the crystal is faster than the timescale of crystallization such that the entire crystal equilibrates with the new melt composition at every time step (Shaw, 2006).

The trace element composition of the equilibrium crystallization C_l^{EC} is calculated by using

$$C_l^{EC} = \frac{C_0}{F + D(1 - F)} \tag{34}$$

2.2.2. Fractional crystallization

Fractional crystallization process will develop if the formed crystals in the melt are prevented from reacting with the melt. It occurs when the formed crystals are separated from the magma chamber without reacting with the melt. Crystals may be separated physically from melt (e.g. gravitational segregation or crystal settling) or alternatively, diffusion in the crystal is so slow with respect to crystallization rate that re-equilibration is precluded.

The trace element composition of the fractional crystallization C_l^{FC} is calculated by using

$$C_l^{FC} = C_0 F^{D-1} \tag{35}$$

2.2.3. In-situ crystallization

In-situ crystallization takes place in the side wall of the magma chamber. This crystallization model was developed instead of the fact that the crystals were gravitationally separated by fractional crystallization from the melt (Langmuir, 1989). The trace element composition of the in-situ crystallization $C_l^{In\text{-}situ}$ is calculated by using

$$C_l^{In\text{-}situ} = C_0 F^{\frac{f(D-1)}{D(1-f)+f}} \tag{36}$$

where f is the fraction of the melt that returns to the magma chamber out of the solidification zone.

2.2.4. Imperfect fractional crystallization

The presence of suspended crystals in the magma chamber greatly influences the change to quantity of compatible elements (Nishimura, 2009). Accordingly, the equilibrium crystallization-imperfect fractional crystallization modeling was developed by assuming the perfect balance between the suspended crystals (δ: fraction (%) of suspended crystals) and melt (Nishimura, 2009).

The trace element composition of the imperfect fractional crystallization $C_l^{EC\text{-}IFC}$ is calculated by using

$$C_l^{EC\text{-}IFC} = C_0 F^{\left(\frac{D}{1-\delta+\delta D}\right)-1} \tag{37}$$

However, volcanic rocks often contain zoned phenocrysts that reflect the absence of solid state equilibrium. Zoned crystallization-imperfect fractional crystallization model was developed by Nishimura (2009). The trace element composition of the zoned crystallization-imperfect fractional crystallization $C_l^{ZC\text{-}IFC}$ is calculated by using

$$C_l^{ZC\text{-}IFC} = C_0\left(F^{\frac{1-\delta}{\delta}} + \frac{(1-\delta)^D}{1-\delta D}\left(F^{D-1} - F^{\frac{1-\delta}{\delta}}\right)\right) \quad (38)$$

where $\delta D \neq 1$ (δD is algebraic multiplication of δ and D) and $\delta \neq 0$ in the case of $\delta D = 1$

$$C_l^{ZC\text{-}IFC} = C_0 F^{D-1}\left(1 + (1-D)\left(1 - \frac{1}{D}\right)\ln F\right) \quad (39)$$

2.2.5. Combined assimilation-fractional crystallization

During the fractional crystallization, the crystallizing magmas may assimilate country rocks. This process is called as assimilation-fractional crystallization (AFC) (DePaolo, 1981). The trace element composition of the assimilation-fractional crystallization C_l^{AFC} is calculated by using

$$C_l^{AFC} = C_0\left(F^{-Z} + \left(\frac{r}{r+D-1}\right)\frac{C_a}{C_0}(1-F^{-Z})\right) \quad (40)$$

$$r = \frac{m_a}{m_c} \quad (41)$$

$$z = \frac{r+D-1}{r-1} \quad (42)$$

in the case of $r + D = 1$

$$C_l^{AFC} = C_0\left(1 + \left(\frac{r}{r-1}\right)\frac{C_a}{C_0} ln(F^{-Z})\right) \quad (43)$$

where C_a is the concentration of the element in the assimilating material, r is the ratio of assimilated material (m_a) to crystallized material (m_c).

Partial melting and closed system differentiation processes (e.g. fractional crystallization) do not change isotope ratios of the initial magma. But, assimilation changes isotope ratios of the melt as an open system process. The isotope ratios of the assimilation-fractional crystallization IC_l^{AFC} is calculated by using

$$IC_l^{AFC} = \frac{\left(\frac{r}{r-1}\right)\left(\frac{C_a}{z}\right)(1-F^{-Z})IC_a + C_0F^{-Z}IC_0}{\left(\frac{r}{r-1}\right)\left(\frac{C_a}{z}\right)(1-F^{-Z}) + C_0F^{-Z}} \quad (44)$$

This can also be written

$$IC_l^{AFC} = \left(1 - \frac{C_0}{C_l^{AFC}}F^{-Z}\right)(IC_a - IC_0) + IC_0 \quad (45)$$

where IC_0 is the isotope ratio of the melt, IC_a is the isotope ratio of the assimilated material. For light stable isotopes such as oxygen (i.e. $\delta^{18}O$) of the assimilation-fractional crystallization δC_l^{AFC} is calculated by using

$$\delta C_l^{AFC} = \left(\delta C_a - \delta C_0 - \frac{\Delta}{r}\right)(1-F^{-Z}) + \delta C_0 \quad (46)$$

it is assumed that $D = 1$ for $\delta^{18}O$
where δC_0 is the stable isotope concentration of the melt, δC_a is the stable isotope concentration of the assimilated material. Δ value is the mineral-melt fractionation factor for stable isotope.

2.2.6. Decoupled assimilation-fractional crystallization

Cribb and Barton (1996) suggested that the assimilation and fractional crystallization are not fully related in a magma system. They argued that the assimilated mass can be separated from the crystallized mass and change independently. This process is defined as Decoupled Assimilation-Fractional Crystallization (FC-A). The trace element composition of the FC-A $\left(C_l^{FC\text{-}A}\right)$ is calculated by using

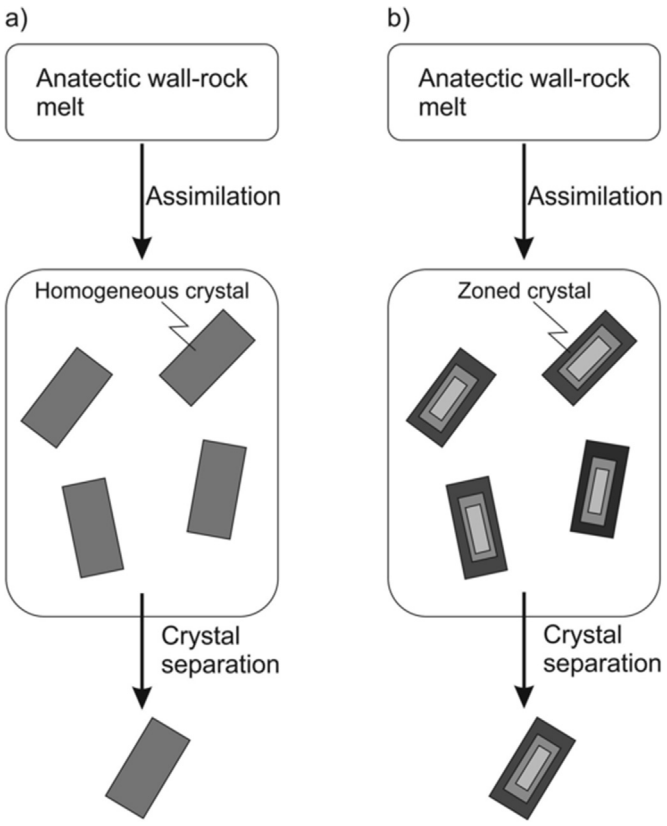

Fig. 3. Schematic illustrations of the A-IFC model proposed by Nishimura (2013). (a) Combined assimilation, perfect equilibrium crystallization, and partial settling. The suspended crystals and liquid remain in perfect chemical equilibrium with each other. (b) Combined assimilation, surface equilibrium crystallization, and partial settling. Chemical zoning is produced by surface equilibrium crystallization of the suspended crystals, but there is no constraint to what extent the crystal is zoned in this model. A certain amount of crystals is suspended for a period that is sufficient to enable re-equilibration with the surrounding liquid in (a), but not in (b).

$$C_l^{FC\text{-}A} = \frac{(C_a r M_c) + C_f(1-M_c)}{F} \quad (47)$$

have to be $F > r$

$$M_c = 1 - \frac{F-r}{1-r} \quad (48)$$

$$C_f = C_0F^{D-1} \quad (49)$$

where M_c is the mass of solid removed, C_f is the result of fractional crystallization.

2.2.7. Assimilation-imperfect fractional crystallization

Conventional geochemical models assume that crystals are removed instantaneously from the magma body as they are produced (Nishimura, 2012). In recent years, the assimilation-imperfect fractional crystallization (A-IFC) model based on a mass-balance calculations has been developed by Nishimura (2012, 2013), showing the effects of the suspended crystals on the whole rock composition in the magma chamber. The A-IFC model considering two end-member cases is different from the conventional AFC model of DePaolo (1981), in which the path of liquid evolution is used to reproduce whole-rock chemical trends. The first end-member is assimilation, perfect equilibrium crystallization (e.g. producing homogeneous crystals) and partial settling (Fig. 3a). The second one is assimilation, zoned crystallization (e.g. fractional crystallization by incomplete chemical reaction, producing zoned crystals), and

partial settling (Fig. 3b). The A-IFC model shows chemical evolution paths of bulk crystals, liquid and magma for both homogeneous and zoned crystal cases (see worked examples).

In the case of homogeneous crystal and $r_a \neq 1$, the trace element compositions ($C^{A\text{-}IFC}$) of the A-IFC are calculated by using

$$C_m^{A\text{-}IFC} = \frac{r_a}{r_a - 1}\frac{C_a}{\acute{\imath}}(1 - F^{-\acute{\imath}}) + C_m^0 F^{-\acute{\imath}} \tag{50}$$

$$C_l^{A\text{-}IFC} = \frac{C_m^{A\text{-}IFC}}{1 - \delta + \delta D} \tag{51}$$

$$C_x^{A\text{-}IFC} = DC_l^{A\text{-}IFC} \tag{52}$$

in the case of homogeneous crystal and $r_a \neq 1$, isotope ratios ($\varepsilon^{A\text{-}IFC}$) of the A-IFC are calculated by using

$$\varepsilon_m = \left(1 - \frac{C_m^0}{C_m^{A\text{-}IFC}}F^{-\acute{\imath}}\right)(\varepsilon_a - \varepsilon_m^0) + \varepsilon_m^0 \tag{53}$$

In this homogeneous crystal case, the isotope ratio of the liquid ε_l and that of the bulk suspended crystals ε_x are identical to ε_m (Nishimura, 2013).

$$\varepsilon_m = \varepsilon_l = \varepsilon_x \tag{54}$$

where $\acute{\imath}$

$$\acute{\imath} = 1 + \frac{D}{(r_a - 1)(1 - \delta + \delta D)} \tag{55}$$

in the case of zoned crystal and $r_a \neq 1$, the trace element compositions ($C^{A\text{-}IFC}$) of the A-IFC are calculated by using

$$C_l^{A\text{-}IFC} = a + (C_l^0 - a)F^{-b} \tag{56}$$

$$C_x^{A\text{-}IFC} = aD - \frac{cD(C_l^0 - a)}{b - c}F^{-b} + \left(C_x^0 - aD + \frac{cD(C_l^0 - a)}{b - c}\right)F^{-c} \tag{57}$$

$$C_m^{A\text{-}IFC} = (1 - \delta)C_l^{A\text{-}IFC} + \delta C_x^{A\text{-}IFC} \tag{58}$$

$$C_l^0 = C_m^0(1 - \delta)^{D-1} \tag{59}$$

$$C_x^0 = C_m^0\frac{1 - (1 - \delta)^D}{\delta} \tag{60}$$

where C_l^0 is the initial elemental concentration of the liquid, C_x^0 is the initial elemental concentration of the suspended crystals. In the case of zoned crystal and $r_a \neq 1$, isotope ratios ($\varepsilon^{A\text{-}IFC}$) of the A-IFC are calculated by using

$$\varepsilon_l = \frac{a\varepsilon_a F^b - a\varepsilon_a + C_l^0\varepsilon_l^0}{aF^b + C_l^0 - a} \tag{61}$$

$$\varepsilon_x = \frac{aD\varepsilon_a - \frac{cD\left(C_l^0\varepsilon_l^0 - a\varepsilon_a\right)}{b-c}F^{-b}}{C_x^{A\text{-}IFC}} + \frac{\left(C_x^0\varepsilon_x^0 - aD\varepsilon_a + \frac{cD\left(C_l^0\varepsilon_l^0 - a\varepsilon_a\right)}{b-c}\right)F^{-c}}{C_x^{A\text{-}IFC}} \tag{62}$$

$$\varepsilon_m = \frac{(1 - \delta)C_l^{A\text{-}IFC}\varepsilon_l + \delta C_x^{A\text{-}IFC}\varepsilon_x}{C_m^{A\text{-}IFC}} \tag{63}$$

where a, b and c

$$a = \frac{r_a C_a}{(\delta r_a + 1 - \delta)D + (1 - \delta)(r_a - 1)} \tag{64}$$

$$b = \frac{(\delta r_a + 1 - \delta)D}{(1 - \delta)(r_a - 1)} + 1 \tag{65}$$

$$c = \frac{\delta r_a + 1 - \delta}{\delta(r_a - 1)} \tag{66}$$

where r_a is ratio of the rate of assimilation to the rate of crystal fractionation, δ weight fraction of suspended crystals, D bulk crystal/liquid partition coefficient for the element.

$C_l^{A\text{-}IFC}$, $C_x^{A\text{-}IFC}$ and $C_m^{A\text{-}IFC}$ are the concentrations of an element in the liquid, bulk suspended crystals and magma, respectively. ε_l, ε_x and ε_m are the isotope ratios in the liquid, crystal and magma, respectively. ε_l^0 is the initial isotopic ratio of the liquid, ε_x^0 is the initial isotopic ratio of the suspended crystals and ε_m^0 is the original isotope ratio in the magma. The isotopic composition of the initial suspended crystal is assumed to be identical to that of the initial liquid ($\varepsilon_x^0 = \varepsilon_l^0$). In the formula, C_a is concentration of the element in the melt derived from wall-rock melting, ε_a is isotope ratio of anatectic wall-rock melt.

2.3. Magma mixing

The magma mixing is defined as interaction of two different magmas giving a mixture with the characteristics of both magmas (Powell, 1984). This process may occur either as a mixture of magma from two different sources or between different compositional zones in the magma chamber. The trace element composition in the magma mixing, $C_{\text{ŋ}}$ is calculated by using

$$C_{\text{ŋ}} = C_A X + C_B(1 - X) \tag{67}$$

The isotope ratios of the magma mixing $IC_{\text{ŋ}}$ is calculated by using

$$IC_{\text{ŋ}} = IC_A\left(\frac{C_A X}{C_{\text{ŋ}}}\right) + IC_B\left(\frac{C_B(1 - X)}{C_{\text{ŋ}}}\right) \tag{68}$$

where C_A is the trace element concentration of the first end member, C_B is the trace element concentration of the second end member. IC_A is the isotope ratio of the first end member, IC_B is the isotope ratio of the second end member, and X is the mixing fraction. The element ratios (e.g. La/Sm-Nb/Zr) of the magma mixing is calculated by using

$$A_1X_1 + A_2X_2 = A \tag{69}$$

$$B_1X_1 + B_2X_2 = B \tag{70}$$

$$C_1X_1 + C_2X_2 = C \tag{71}$$

$$D_1X_1 + D_2X_2 = D \tag{72}$$

have to be $X_1 + X_2 = 1$

$$X_1 = \frac{A - A_2}{A_1 - A_2} = \frac{B - B_2}{B_1 - B_2} = \frac{C - C_2}{C_1 - C_2} = \frac{D - D_2}{D_1 - D_2} \tag{73}$$

where A_1, B_1, C_1 and D_1 are the trace element concentration of the first end member. A_2, B_2, C_2 and D_2 are the trace element concentration of the second end member. X_1 and X_2 are the mixing rate.

$$\alpha(x\text{-}axis) = \frac{A}{B}\ and\ \beta(y\text{-}axis) = \frac{C}{D} \tag{74}$$

the hyperbolic value of the resulting curve can be calculated by the following formula

$$\beta(A_2D_1 - A_1D_2) + \alpha(B_2C_1 - B_1C_2) + \alpha\beta(D_2B_1 - D_1B_2) + (C_2A_1 - C_1A_2) = 0 \tag{75}$$

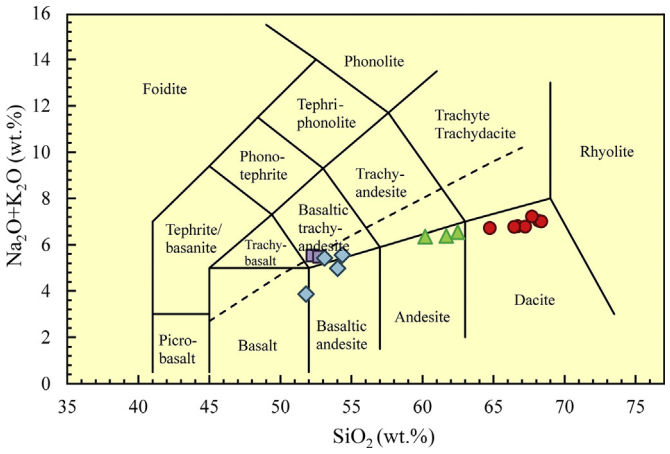

Fig. 4. Total alkali-silica diagram (Le Bas et al., 1986) with the dashed line separating alkaline-subalkaline compositions (Irvine and Baragar, 1971). Data used in this classification were entered in "Group 1 to 4" of "Geochemical data" sheet in PetroGram, and are from Gündüz (2017) and Asan et al. (2019).

in the case that the result is "0" magma mixture model with linear direction will be formed (Shaw, 2006).

3. Program structure

PetroGram is a Microsoft® Excel© workbook that is specifically designed for the needs and demands of researchers working on magmatic petrology. It has been designed on ten Excel sheets: "Geochemical data", "Parameters", "Classification", "Tectonic setting", "Models", "Spiders", "Isotopes", "XYZ plot", "Assimilation-IFC" and "Output". In the following, we summarize the function of the sheets by combining some of them.

3.1. Geochemical data

The data (e.g. major oxide (wt.%), trace element (ppm), isotope ratio and age in Ma) should be entered into the rows and columns of the groups within the "Geochemical data" spreadsheet. In addition, you can easily change contents of the yellow boxes which are for algebraic calculations in the "OTHERS" section.

Following the data entry, basic geochemical calculations (Mg#, Eu/Eu*, ε_{Sr}, ε_{Nd}, etc.) and CIPW (%) results are automatically calculated by the program within the "Geochemical data" spreadsheet. Finally, representations of the each sample on the diagrams can be done by entering "0" or "1" values into the cell under the sample number.

3.2. Parameters

"Parameters" spreadsheet is mainly designed for the entrance of values used in "Models" spreadsheet. All values (i.e. source rocks, normalizing values and *Kd*'s) can be modified in the spreadsheet according to the purpose of users. In addition, inverse geochemical modeling can be performed by calculating partial melting degrees (%*F*) and by entering appropriate data in this spreadsheet.

3.3. Classification and tectonic setting

It is possible to use important rock classifications such as total alkali (K_2O + Na_2O)-silica (SiO_2) diagram (Le Bas et al., 1986) and tectonic setting diagrams within these spreadsheet (Fig. 4). The samples on these diagrams can be easily removed through the check boxes in the rock groups of "Geochemical data". The symbol of samples on the diagrams can be changed by using properties of Excel.

3.4. Spiders

In magma series, the enrichment and depletion of elements can be seen by creating spider diagrams. It is also possible to compare the rocks derived from different mantle sources and the magmatic rocks representing different tectonic setting. "Spiders" sheet is flexible that users can arrange their element order. The normalizing values of each groups can be selected from the drop-down menu to create spider diagrams. The mostly used normalizing values (MORB, OIB, Chondrite, Primitive mantle etc.) have already been entered as default in PetroGram, but users can enter their values by replacing with the entered ones in "Parameters" sheet.

3.5. Models

The magmatic processes such as partial melting, fractional crystallization, assimilation-fractional crystallization and magma mixing can be easily modelled from the "Models" spreadsheet (Fig. 5). Bivariate X-Y diagrams can also be created in the same spreadsheet.

The "Models" sheet contains four sections and two diagrams. These are models of Partial Melting, Rock Groups, X-Y Diagrams and Modeling on the X-Y Diagrams. The diagrams are divided into multi-variate and multi-element. Models are made by using different methods on each diagram. The axes of the diagrams can be set up as linear or logarithmic scales from the Excel's axis options. The groups of sample are chosen by using "Rocks Groups" sections on the related check boxes in order to plot them on the diagrams (Fig. 5-1).

In order to create forward partial melting models, you need to choose source rocks and the partition coefficient (*Kd*) in the combo box (Fig. 5-2a). The source rock compositions and partition coefficient can be changed from the "Parameters" spreadsheet. Also the names of the normalizing values in the combo box can be updated by users from the "Parameters" spreadsheet. The fractions (F) and normalizing values of the models can be changed in the combo boxes (Fig. 5-2b, 5-2c). You need to enter mineral modes in the related Excel cells at "Models" spreadsheet (Fig. 5-2d). In order to exhibit of the partial melting models on the diagrams, you need to choose the related check boxes (Fig. 5-2e). The proportions of mixing line can be shown by choosing in the combo box (Fig. 5-2f) which is related to partial melting models on the X-Y diagram. The melt fraction (*X*) of dynamic melting can be calculated by entering of the porosity of mantle (ϕ_v), density of solid (ρ_s) and density of liquid (ρ_f) from the related spin buttons (Fig. 5-2g, 5-2h, 5-2i).

For inverse partial melting model, you need first to enter two samples the best representing your melt composition from your data set and bulk partition coefficients (*D*) in "Parameters" spreadsheet. Then, F_1 and F_2 values for inverse batch melting, and X_1 and X_2 values for inverse dynamic melting need to be specified in "Parameters" spreadsheet. Lastly, the *F* value for inverse batch and dynamic melting needs to be entered based on the calculation of the average F_1 and F_2 by the program. The results of calculation can be exhibited by using of check boxes (Fig. 5-2j) on the multi-element diagram in the "Models" spreadsheet.

The crystallization processes and magma mixing can easily be modelled by using "Modeling on the X-Y Diagrams" section in the "Models" spreadsheet. First, you need to select starting sample or composition (C_0) from the check box (Fig. 5-4a). The starting composition can be chosen as samples or melting results from the option buttons and combo boxes (Fig. 5-4b, 5-4c). Bulk partition coefficients (*D*) have to be entered for all selecting elements in the related Excel cells where are in below of the starting compositions (Fig. 5-4d). After determining the starting composition, the bulk coefficient and *F* values (Fig. 5-4e), the desired models can be selected by choosing the related check boxes (Fig. 5-4f). For assimilation models, you need to choose an assimilant material (C_a) from related combo boxes (Fig. 5-4g). The "δ" (Fig. 5-4h) value for the EC-IFC and ZC-IFC, the "f" value (Fig. 5-4i) for the In-situ crystallization and the "r" value (Fig. 5-4j) for the assimilation can be set up by using related spin buttons. Magma mixing can be modelled by

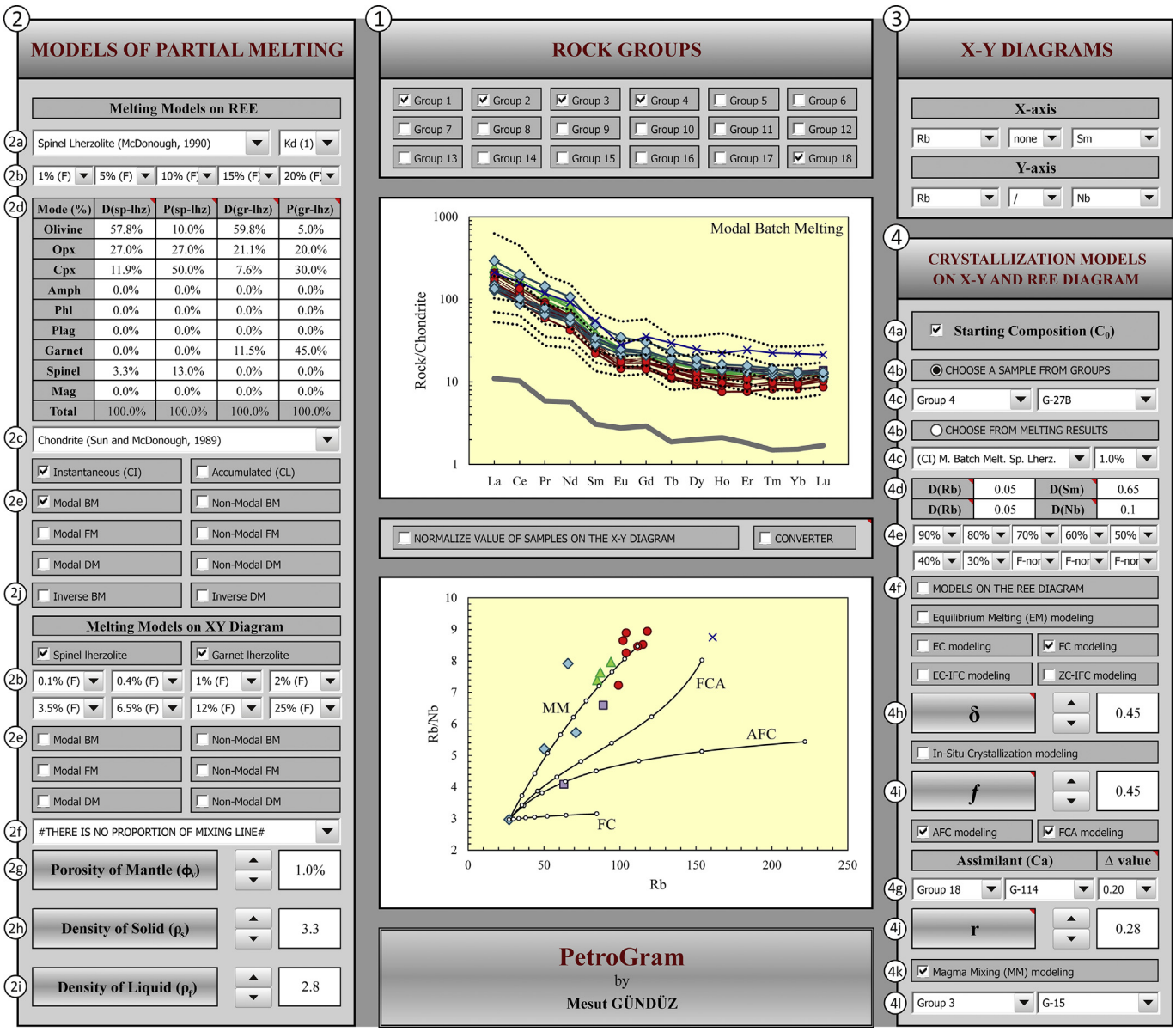

Fig. 5. Screenshots of "Models" sheet of PetroGram showing the main panels: Models of Partial Melting, Rocks Groups, X-Y Diagrams and Modeling on the X-Y Diagrams.

choosing related buttons (Fig. 5-4k) and second sample (Fig. 5-4l). Also it can be modelled on the REE diagram by choosing the percentage of mixing ratio (Fig. 5-4e).

3.6. Isotopes and XYZ plot

The isotope correlation diagrams given in the "Isotope" spreadsheet are based on the isotope ratios of Zindler and Hart (1986) and Hofmann (2007). The samples on these diagrams can be easily removed through the check boxes in the rock groups. They can also be created from multivariate diagrams in the "Models" spreadsheet. On the other hand, triangle and bivariate diagrams can be created by using in "XYZ plot" spreadsheet. In order to change the elements on a triangle or bivariate diagram, you need to click the combo boxes in spreadsheet.

3.7. Assimilation-IFC

Assimilation-imperfect fractional crystallization (A-IFC) modeling is an assimilation model used to understand the effects of suspended crystals on element abundances in the magma chamber. When the *x*-axis is selected as a trace element, the *y*-axis should be an isotope value of this trace element to create an A-IFC model. In this sheet, after the entering of initial (C_m^0 and ε_m^0) and assimilant (C_a and ε_a) values, A-IFC modeling can be created by entering the ratio of the rate of assimilation to the rate of crystal fractionation (r_a), weight fraction of suspended crystals (δ) and bulk crystal/liquid partition coefficient for the element (D). If $r_a < 1$, the Final F have to be $F < 1$ and $r_a > 1$, the Final F have to be $F > 1$. When $r_a = 1$, the Final M_a/M_m value is required (Nishimura, 2013) (see worked examples).

3.8. Output

The "Output" spreadsheet consist of partial melting results. The results mainly occur as modal and non-modal partial melting and residual solid, total residual. The analytical data can be used by choosing in the X-Y or REE diagrams. The porosity (ϕ_m) value of the dynamic melting data can be changed within the "Models" spreadsheet.

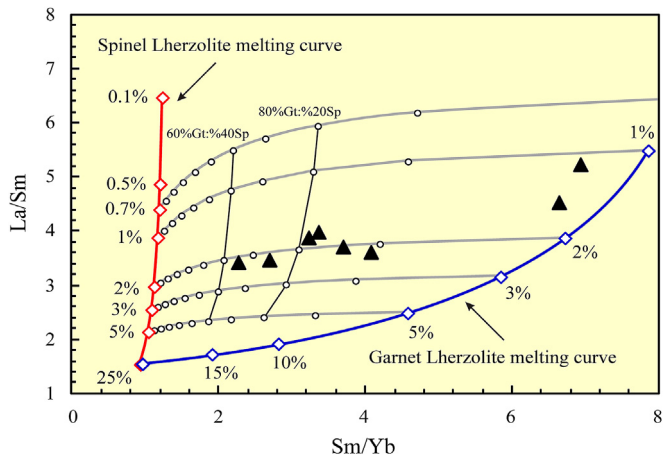

Fig. 6. Non-Modal Batch melting model produced by PetroGram on the Sm/Yb vs. La/Sm bivariate plot for the Karacadağ volcano basalts, Eastern Anatolia. Please see Fig. 14 of Özdemir and Güleç (2014) for comparison. Data used in this modeling were entered in "Group 7" of "Geochemical data" sheet in PetroGram.

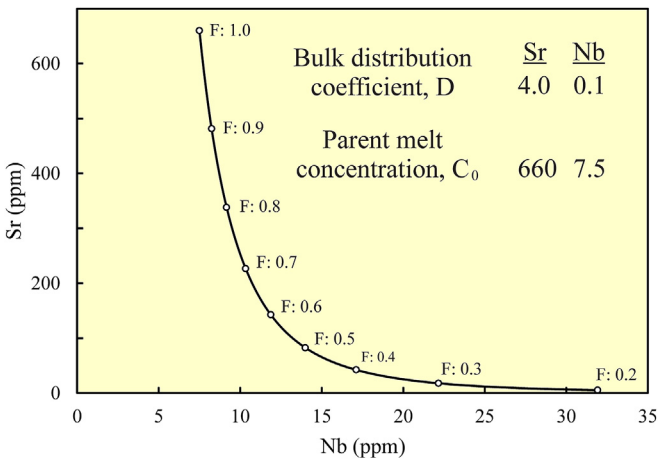

Fig. 7. FC model produced by PetroGram on the Nb vs. Sr bivariate plot for the Pahranagat Formation pumices, Nevada. Please see fig. 15 of Best et al. (1995) for comparison. Data used in this modeling were shown on this figure.

4. Worked examples

The best way to test and learn PetroGram is to remodel the data from the published studies. Here we reprocess examples of the melting, fractional crystallization and assimilation by utilizing PetroGram.

For forward partial melting model, we reprocess here the Karacadağ volcano (Eastern Anatolia, Turkey). Özdemir and Güleç (2014) showed that basaltic rocks from the Karacadağ volcano are consistent with various degrees of melting between 1% and 2% and have a garnet peridotite contribution of more than 80% in their petrogenesis based on the non-modal batch melting. To construct the partial melting model in PetroGram, you need to enter spinel and garnet lherzolite values into "Parameters" sheet and the Karacadağ volcano data into "Geochemical data" sheet. In "Parameters" sheet, Kd_1 and Kd_2 are already entered for partial melting models. But, the users can manually change Kd values if desired. Next, you should go to "Models" sheet to construct bivariate X-Y plot. Then, the element ratios Sm/Yb and La/Sm should be chosen for X- and Y-axis, respectively, using the drop-down menu at the upper right corner. At this step, you need to click instantaneous (C_I) or accumulated (C_L) checkbox and to define mineral and melting modes to be automatically calculated D and P values by the program. You also need to select F values from the drop-down menu and to click the spinel and garnet lherzolite check boxes at the middle of left panel. Lastly, model vectors will be shown when you click the Non-Modal BM checkbox at the middle of right panel (Fig. 6). You can also plot mixing lines on the same plot by clicking selecting this feature.

Estimation for the mantle composition and melting degrees of the Honolulu volcanics from Hawaii (USA) appears to provide a good example for inverse dynamic melting of Zou and Zindler (1996). To recalculate the partial melting degrees and mantle source compositions by using inverse dynamic melting in PetroGram, you need to enter D values for REE (rare earth elements) and two basaltic samples from dataset into "Parameters" sheet. The program calculates Q and ϕ_m values. By using these values, you should manually calculate X_1 and X_2 values from the Newton-Raphson method or use the given excel sheet as a separate file that we called "IBM_IDM Calculator" based on the concentration ratio method of Maaløue (1994). In the left panel of IDM sheet of this calculator, the users should enter concentration ratios (Q) of highly incompatible elements (e.g. "Th" as "Q_A" for the selected case) and less incompatible elements (e.g. "REEs" as "Q_B") from two basaltic samples, their bulk partition coefficients (D_A, D_B) and mass porosity (ϕ_m). Then, the users need to click "Reset" and "Results" button respectively, and the calculator will produce X_1 and X_2 values to be entered in PetroGram. At this step, the user should check whether the Q_n value in the right panel approximately equals to the Q_B in left panel. If not, the users need to decrease the range between Initial-X_1 and Final-X_1 in the left panel by considering the calculated X_1 value in the right panel, for example if the calculated X_1 value is 1.51%, Initial-X_1 and Final-X_1 may range from 1 to 2. Now, the users have X_1 and X_2 values produced by "IBM_IDM Calculator" to be entered into PetroGram. After entering X_1 and X_2 values into PetroGram, the program calculates F_1 and F_2 values. You need manually to enter the F value ranging between F_1 and F_2 values in "Parameters" sheet. Then, you need to go to "Models" sheet to change the porosity of mantle (ϕ_v), density of solid (ρ_s) and liquid (ρ_f). The calculated C_0 values

Table 2
Comparison of inverse dynamic melting (IDM) model results between Zou and Zindler (1996)* and PetroGram.

	Zou and Zindler (1996)						PetroGram
	D	Sample 1	Sample 2	Q	F_1	F_2	C_0	C_0
Th	0.0010	9.6	2.1	4.571				
La	0.0021	90.1	21	4.290	1.9%	7.7%	1.59	1.614
Ce	0.0041	160	44	3.636	1.2%	6.0%	3.11	3.152
Nd	0.0095	66.7	22	3.032	1.8%	7.7%	1.63	1.649
Sm	0.0180	15.2	5.91	2.572	2.3%	9.2%	0.50	0.500
Eu	0.0228	4.49	1.98	2.268	2.2%	8.8%	0.17	0.169
Tb	0.0330	1.64	0.81	2.025	2.5%	9.7%	0.08	0.078
Yb	0.2644	1.8	1.6	1.125	2.8%	11.0%	0.50	0.495
Lu	0.4460	0.26	0.25	1.040	2.0%	8.2%	0.12	0.118
Ave.					2.1%	8.5%		

*ϕ_v = 1.0%, ρ_s = 3.3 and ρ_f = 2.8. Data used in this modeling were entered in "Dynamic Melting Inverse Geochemical Modeling (IDM)" of "Parameters" sheet in PetroGram.

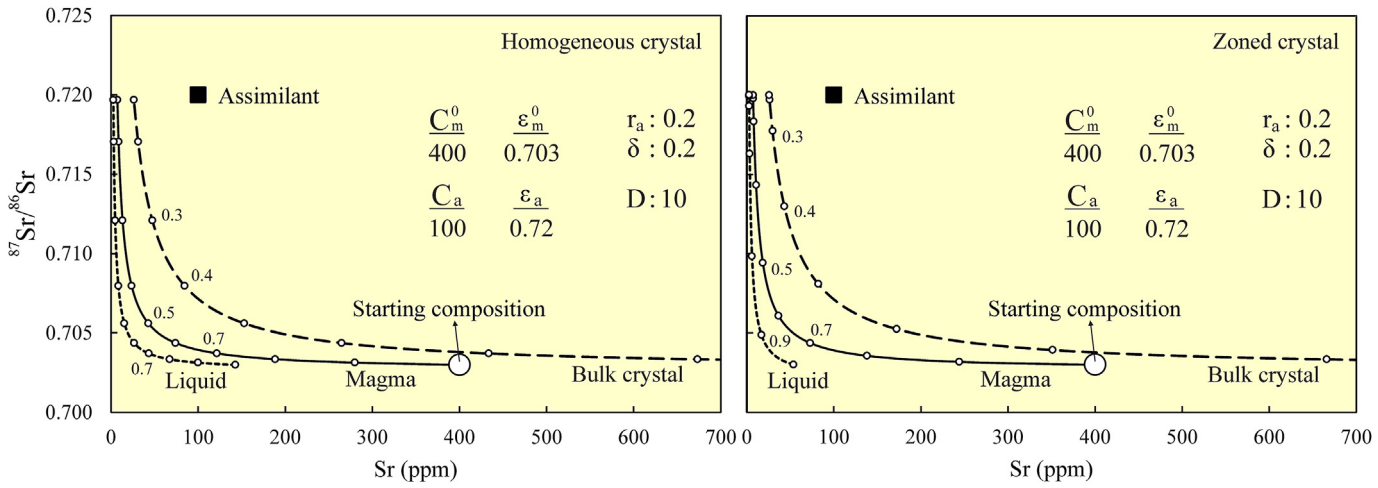

Fig. 8. Sr vs. $^{87}Sr/^{86}Sr$ plot showing A-IFC model (homogeneous or zoned crystal) produced by PetroGram. Please see fig. 4 of Nishimura (2013) for comparison. Data used in this modeling were already entered as default in "Assimilation-IFC sheet" of PetroGram.

are shown in "Parameters" sheet. The comparison of inverse dynamic melting (IDM) model results between those of Zou and Zindler (1996) and PetoGram is given Table 2.

For fractional crystallization, we remodel geochemical variations in the pumices from the Pahranagat Formation, Nevada. The pumices experienced fractional crystallization of two feldspars, quartz, biotite and Fe-Ti oxides were modelled by Best et al. (1995) on the Nb-Sr bivariate plot with starting compositions (C_0) for Sr: 660 ppm and Nb: 7.5 ppm, bulk partition coefficients (D) for Sr: 4.0 and Nb: 0.1. To reproduce the FC model on Nb-Sr plot one should enter or copy and paste the Nb-Sr data into "Geochemical data" sheet of PetroGram. After entering data, one needs to go to "Models" sheet to construct X-Y diagram. Then, the elements Nb and Sr should be chosen for X- and Y-axis, respectively, using the drop-down menu at the upper right corner. Next, one should click "Starting Composition" (C_0) and choose a sample from groups for parental magma. One can also choose a starting composition from any melting results if previously produced in PetroGram. At this step, in the middle of right panel of the sheet, you need to enter manually D values for each element used in modeling. F values should be defined from the drop down menu just below D values. Lastly, a model vector for which you entered D values will be shown when you click the FC (Fractional Crystallization) checkbox at middle of right panel of the sheet (Fig. 7). The users can also plot the other model trajectories (e.g. EC, AFC, FCA, magma mixing etc.) on the same bivariate plot by clicking the relevant checkbox.

Another model reproduced by PetroGram is the A-IFC model of Nishimura (2012, 2013). For this, we reprocessed a conceptual model on the Sr vs. $^{87}Sr/^{86}Sr$ bivariate plot given by Nishimura (2012, 2013) using initial magma and assimilant composition of DePaolo (1981). To produce Assimilation-IFC model in PetroGram, one needs to go to "Assimilation-IFC" sheet to construct X-Y diagram. Then, the trace element Sr and isotope ratio $^{87}Sr/^{86}Sr$ should be chosen for X- and Y-axis, respectively, using the drop-down menu at the upper right corner. At this step, you need to enter manually the relevant values (e.g. r_a, C_a, D etc.) used in A-IFC modeling at the left panel of the sheet. Lastly, a model trajectory for which you entered the relevant values will be shown when you click the checkboxes (i.e. Liquid, Bulk crystals, Magma) at lower corner of left panel of the sheet (Fig. 8).

5. Conclusions

PetroGram is an Excel© based, open and free magmatic petrology program. PetroGram is mainly designed to model petrological processes (e.g. partial melting, crystallization, assimilation and magma mixing), but it can also be used for classical geochemical plots (e.g. Rock classification, REE, Spider, Geotectonic setting diagrams etc.) and calculations (Mg#, Eu/Eu*, ε_{Sr}, ε_{Nd}, CIPW etc.). The main difference in PetroGram from the existing programs is that it can produce inverse geochemical models in addition to traditional forward geochemical models. The produced graphical and numerical output from the program can easily be exported as "gif/jpeg/tiff" files and tables.

Declaration of competing interest

The authors declare that they have no known competing financial interests or personal relationships that could have appeared to influence the work reported in this paper.

Acknowledgments

The authors thank to the Associate Editor Dr. Stijn Glorie, and Dr. Paolo Sossi and an anonymous reviewer for their critical and constructive comments that improved the quality of this paper and PetroGram.

Appendix A. Supplementary data

Supplementary data to this article can be found online at https://doi.org/10.1016/j.gsf.2020.06.010.

References

Annen, C., Blundy, J.D., Sparks, R.S.J., 2008. The sources of granitic melt in Deep Hot Zones. Earth Environ. Sci. Trans. Royal Soc. Edinburgh 97, 297–309.
Asan, K., Kurt, H., Gündüz, M., Gençoğlu Korkmaz, G., Morgan, G., 2019. Geology, geochronology and geochemistry of the Miocene Sulutas volcanic complex, Konya-Central Anatolia: genesis of orogenic and anorogenic rock associations in an extensional geodynamic setting. Int. Geol. Rev. 61, 1–32.
Asimow, P., Ghiorso, M.S., 1998. Algorithmic modifications extending MELTS to calculate subsolidus phase relations. Am. Mineral. 83 (9), 1127–1132.
Barbarin, B., 2005. Mafic magmatic enclaves and mafic rocks associated with some granitoids of the central Sierra Nevada batholith, California: nature, origin, and relations with the hosts. Lithos 80 (1), 155–177.
Barker, F., Wones, D.R., Sharp, W.N., Desborough, G.A., 1975. The Pikes Peak Batholith, Colorado Front Range, and a model for the origin of the gabbro-anorthosite-syenite-potassic granite suite. Precambrian Res. 2, 97–160.
Best, M.G., Christiansen, E.H., Deino, A.L., Grommé, C.S., Tingey, D.G., 1995. Correlation and emplacement of a large, zoned, discontinuously exposed ash flow sheet: the $^{40}Ar/^{39}Ar$ chronology, paleomagnetism, and petrology of the Pahranagat Formation, Nevada. J. Geophys. Res.: Solid Earth 100, 24593–24609.
Cribb, J.W., Barton, M., 1996. Geochemical effects of decoupled fractional crystallization and crustal assimilation. Lithos 37, 293–307.
Danyushevsky, L.V., Plechov, P.Y., 2011. Petrolog3: integrated software for modeling crystallization processes. G-cubed 12 (7), 1–32.
DePaolo, D.J., 1981. Trace element and isotopic effect of combined wallrock assimilation and fractional crystallization. Annu. Rev. Earth Planet Sci. 53, 189–202.

Ersoy, Y., 2013. PETROMODELER (Petrological Modeler): a Microsoft® Excel© spreadsheet program for modelling melting, mixing, crystallization and assimilation processes in magmatic systems. Turk. J. Earth Sci. 22, 115–125.
Ersoy, Y., Helvacı, C., 2010. FC-AFC-FCA and mixing modeler: a Microsoft Excel & spreadsheet program for modeling geochemical differentiation of magma by crystal fractionation, crustal assimilation and mixing. Comput. Geosci. 36, 383–390.
Gast, P.W., 1968. Trace element fractionations and the origin of tholeiitic and alkaline magma types. Geochem. Cosmochim. Acta 32, 1057–1086.
Ghiorso, M.S., Sack, R.O., 1995. Chemical mass transfer in magmatic processes IV. A revised and internally consistent thermodynamic model for the interpolation and extrapolation of liquid-solid equilibria in magmatic systems at elevated temperatures and pressures. Contrib. Mineral. Petrol. 119, 197–212.
Gündüz, M., 2017. Geochronology, Mineral Chemistry, Elemental and Isotope Geochemistry of the Neogene Volcanic Rocks Outcropped Around Sarayköy-Sille-Tatköy Küçükmuhsine (NW, Konya). Selçuk University, Konya, p. 109.
Helz, R., 1980. Crystallization history of Kilauea Iki lava lake as seen in drill core recovered in 1967-1979. Bull. Volcanol. 43, 675–701.
Hofmann, A.W., 2007. Sampling mantle heterogeneity through oceanic basalts: isotopes and trace elements. In: Holland, H.D., Turekian, K.K. (Eds.), Treatise on Geochemistry. Pergamon, Oxford, pp. 1–44.
Irvine, T.N., Baragar, W.R.A., 1971. A guide to the chemical classification of the common volcanic rocks. Can. J. Earth Sci. 8, 523–548.
Janoušek, V., Farrow, C.M., Erban, V., 2003. GCDkit: new PC software for interpretation of whole-rock geochemical data from igneous rocks. Geochem. Cosmochim. Acta 67, 186.
Janoušek, V., Farrow, C.M., Erban, V., 2006. Interpretation of whole-rock geochemical data in igneous geochemistry: introducing Geochemical Data Toolkit (GCDkit). J. Petrol. 47, 1255–1259.
Kamenetsky, V.S., Kamenetsky, M.B., Maas, R., 2011. New identity of the kimberlite melt: constraints from unaltered diamondiferous Udachnaya-east pipe kimberlite, Russia. In: Chen, D. (Ed.), Advances in Data, Methods, Models and Their Applications in Geoscience. InTech Open Access Publisher, pp. 181–214.
Keskin, M., 2002. FC-Modeler: a Microsoft® Excel© spreadsheet program for modeling Rayleigh fractionation vectors in closed magmatic systems. Comput. Geosci. 28, 919–928.
Keskin, M., 2013. AFC-Modeler: a Microsoft® Excel© workbook program for modelling assimilation combined with fractional crystallization (AFC) process in magmatic systems by using equations of DePaolo (1981). Turk. J. Earth Sci. 22, 304–319.
Kumar, S., 2014. Magmatic processes: review of some concepts and models. In: Kumar, S., Singh, R.N. (Eds.), Modelling of Magmatic and Allied Processes. Society of Earth Scientists Series. Springer, Cham, pp. 1–22. https://doi.org/10.1007/978-3-319-06471-0_1.
Langmuir, C.H., 1989. Geochemical consequences of in situ crystallization. Nature 340, 199–205.
Langmuir, C.H., Bender, J.F., Bence, A.E., Hanson, G.N., Taylor, S.R., 1977. Petrogenesis of basalts from the FAMOUS-area, Mid-Atlantic ridge. Earth Planet Sci. Lett. 36, 133–156.
Le Bas, M.J., Le Maitre, R.W., Streckeisen, A., Zanettin, B., 1986. A chemical classification of volcanic rocks based on total alkali-silica diagram. J. Petrol. 27, 745–750.
Lu, Y.F., 2004. GeoKit: a geochemical toolkit for Microsoft excel. Geochem. Cosmochim. Acta 33 (5), 459–464.
Maaløue, S., 1994. Estimation of the degree of partial melting using concentration ratios. Geochem. Cosmochim. Acta 58, 2519–2525.
Marrett, R., Emerman, S.H., 1992. The relations between faulting and mafic magmatism in the Altiplano-Puna plateau (central Andes). Earth Planet Sci. Lett. 112, 53–59.
Marshak, S., 2008. Earth: Portrait of a Planet, 3 ed. W.W. Norton & Company, New York.
McKenzie, D., 1984. The generation and compaction of partially molten rock. J. Petrol. 25, 713–765.
McKenzie, D., 1985a. ^{230}Th-^{238}U disequilibrium and the melting processes beneath ridge axes. Earth Planet Sci. Lett. 72, 149–157.
McKenzie, D., 1985b. The extraction of magma from the crust and mantle. Earth Planet Sci. Lett. 74, 81–91.
McKenzie, D., Bickle, M.J., 1988. The volume and composition of melt generated by extension of the lithosphere. J. Petrol. 29, 625–679.
Nishimura, K., 2009. A trace-element geochemical model for imperfect fractional crystallization associated with the development of crystal zoning. Geochem. Cosmochim. Acta 73, 2142–2149.
Nishimura, K., 2012. A mathematical model of trace element and isotopic behavior during simultaneous assimilation and imperfect fractional crystallization. Contrib. Mineral. Petrol. 164, 427–440.
Nishimura, K., 2013. AIFCCalc: an Excel spread sheet for modeling simultaneous assimilation and imperfect fractional crystallization. Comput. Geosci. 51, 410–414.
Özdemir, Y., Güleç, N., 2014. Geological and geochemical evolution of the Quaternary Süphan stratovolcano, eastern Anatolia, Turkey: evidence for the lithosphere-asthenosphere interaction in post-collisional volcanism. J. Petrol. 55, 37–62.
Petrelli, M., Poli, G., Perugini, D., Peccerillo, A., 2005. PetroGraph: a new software to visualize, model, and present geochemical data in igneous petrology. G-cubed 6 (7), 1–15.
Powell, R., 1984. Inversion of the assimilation and fractional crystallization (AFC) equations; characterization of contaminants from isotope and trace element relationships in volcanic suites. J. Geol. Soc. 141, 447–452.
Rollinson, H.R., 1993. Using Geochemical Data: Evaluation, Presentation, Interpretation. Longman, Essex, p. 352.
Schilling, J.G., Winchester, J.W., 1967. Rare-earth fractionation and magmatic processes. In: Runcorn, S.K. (Ed.), Mantle of the Earth and Terrestrial Planets. Interscience Publication, pp. 267–283.
Shaw, D.M., 1970. Trace element fractionation during anatexis. Geochem. Cosmochim. Acta 34, 237–243.
Shaw, D.M., 2000. Continuous (dynamic) melting theory revisited. Can. Mineral. 38, 1041–1063.
Shaw, D.M., 2006. Trace Element in Magma A Theoretical Treatment. Cambridge University Press, Cambridge.
Shirley, D.N., 1987. Differentiation and compaction of the palisades sill, New Jersey. J. Petrol. 28, 835–865.
Sims, K.W.W., DePaolo, D.J., Murrell, M.T., Baldridge, W.S., Goldstein, S., Clague, D., Jull, M., 1999. Porosity of the melting zone and variations in the solid mantle upwelling rate beneath Hawaii: inferences from ^{238}U-^{230}Th-^{226}Ra and ^{235}U-^{231}Pa disequilibria. Geochem. Cosmochim. Acta 63, 4119–4138.
Su, Y., Langmuir, C.H., Asimow, P.D., 2003. PetroPlot: a plotting and data management tool set for Microsoft Excel: PETROPLOT. G-cubed 4 (3), 1030.
Wang, X., Ma, W., Gao, S., Ke, L., 2008. GCDPlot: an extensible microsoft excel VBA program for geochemical discrimination diagrams. Comput. Geosci. 34 (12), 1964–1969.
Wilson, M., 1989. Igneous Petrogenesis: A Global Tectonic Approach. Unwin Hyman, London.
Yu, Q.-Y., Bagas, L., Yang, P.-H., Zhang, D., 2019. GeoPyTool: a cross-platform software solution for common geological calculations and plots. Geosci. Front. 10, 1437–1447.
Zhou, J., Li, X., 2006. GeoPlot: an Excel VBA program for geochemical data plotting. Comput. Geosci. 32 (4), 554–560.
Zindler, A., Hart, S.R., 1986. Chemical geodynamics. Annu. Rev. Earth Planet Sci. 14, 493–571.
Zou, H., 1998. Trace element fractionation during modal and nonmodal dynamic melting and open-system melting: a mathematical treatment. Geochem. Cosmochim. Acta 62, 1937–1945.
Zou, H., 2000. Modeling of trace element fractionation during non-modal dynamic melting with linear variations in mineral/melt distribution coefficients. Geochem. Cosmochim. Acta 64, 1095–1102.
Zou, H., 2007. Quantitative Geochemistry. Imperial College Press, London.
Zou, H., Reid, M.R., 2001. Quantitative modeling of trace element fractionation during incongruent dynamic melting. Geochem. Cosmochim. Acta 65, 153–162.
Zou, H., Zindler, A., 1996. Constraints on the degree of dynamic partial melting and source composition using concentration ratios in magmas. Geochem. Cosmochim. Acta 60, 711–717.